

Role for the NR2B subunit of the *N*-methyl-D-aspartate receptor in mediating light input to the circadian system

L. M. Wang,¹ A. Schroeder,¹ D. Loh,¹ D. Smith,¹ K. Lin,¹ J. H. Han,¹ S. Michel,^{1,*} D. L. Hummer,^{2,4} J. C. Ehlen,^{2,†} H. E. Albers^{2,3,4} and C. S. Colwell¹

¹Department of Psychiatry and Biobehavioral Sciences, University of California — Los Angeles, 760 Westwood Plaza, Los Angeles, CA 90024-1759, USA

²Department of Biology,

³Department of Psychology and

⁴Center for Behavioral Neuroscience, Georgia State University, Atlanta, GA, USA

Keywords: Ca²⁺, circadian rhythms, fura2, ifenprodil, mice, suprachiasmatic nucleus, Syrian hamsters

Abstract

Light information reaches the suprachiasmatic nucleus (SCN) through a subpopulation of retinal ganglion cells that utilize glutamate as a neurotransmitter. A variety of evidence suggests that the release of glutamate then activates *N*-methyl-D-aspartate (NMDA) receptors within the SCN and triggers a signaling cascade that ultimately leads to phase shifts in the circadian system. In this study, we first sought to explore the role of the NR2B subunit in mediating the effects of light on the circadian system of hamsters and mice. We found that localized microinjection of the NR2B subunit antagonist ifenprodil into the SCN region reduces the magnitude of light-induced phase shifts of the circadian rhythm in wheel-running activity. Next, we found that the NR2B message and levels of phospho-NR2B vary with time of day in SCN tissue using semiquantitative real-time polymerase chain reaction and western blot analysis, respectively. Functionally, we found that blocking the NR2B subunit with ifenprodil significantly reduced the magnitude of NMDA currents recorded in SCN neurons. Ifenprodil also significantly reduced the magnitude of NMDA-induced Ca²⁺ changes in SCN cells. Together, these results demonstrate that the NR2B subunit is an important component of NMDA receptor-mediated responses within SCN neurons and that this subunit contributes to light-induced phase shifts of the mammalian circadian system.

Introduction

Circadian oscillators generate daily rhythms with a period close, but not equal, to 24 h. In order to function adaptively, these near-24-h rhythms must be entrained to the exact 24-h physical world. The daily cycle of light and dark is the dominant cue responsible for entrainment. In mammals, these photic signals that regulate the circadian system are detected, at least in part, by a distinct subset of retinal ganglion cells that contain the novel photopigment melanopsin and are directly light sensitive (Berson, 2003). The axons of these retinal ganglion cells form the retinohypothalamic tract (RHT), which terminates within the suprachiasmatic nucleus (SCN). Many SCN neurons contain the molecular machinery that enables them to generate circadian oscillations (Hastings & Herzog, 2004). There is a variety of evidence suggesting that the amino acid glutamate is a transmitter at the RHT/SCN synaptic connection (Morin & Allen, 2006). The release of glutamate is detected by both *N*-methyl-D-aspartate (NMDA) and amino-methyl propionic acid/kainate receptors (Morin & Allen, 2006). Thus, the properties of the NMDA

receptors expressed in the SCN will influence how the circadian system responds to light.

The NMDA receptor is a multimeric protein complex that consists of NR1 subunits and one or more NR2 subunits (McBain & Mayer, 1994; Cull-Candy *et al.*, 2001). The presence of different NR2 subunits results in NMDA receptors with distinct pharmacological and kinetic properties. For example, NMDA receptors that contain the combination of NR1 and NR2B subunits are blocked by MK-801, have slower kinetics and are highly permeable to Ca²⁺ (McBain & Mayer, 1994). This latter point is important for the transduction of the retinal input to SCN neurons as a variety of evidence indicates that the NMDA-induced Ca²⁺ influx is likely to be the first step in a cascade of events that ultimately leads to phase shifts in the circadian system (e.g. Ding *et al.*, 1994, 1997; Obrietan *et al.*, 1998; Colwell, 2001). Furthermore, rapid regulatory changes in subunit composition as well as post-translational modifications to these subunits could underlie diurnal rhythms in NMDA-mediated currents and Ca²⁺ responses measured in SCN neurons (Colwell, 2001; Pennartz *et al.*, 2001). The transcript coding for the NR2B subunit of the NMDA receptor is present in the SCN (O'Hara *et al.*, 1995; Moriya *et al.*, 2000; Matsushita *et al.*, 2006) and one study has shown a physiological role for this subunit (Kim *et al.*, 2006). NMDA receptors containing the NR2B subunit can be selectively inhibited with ifenprodil (Williams, 1993, 2001). This pharmacological agent gives us a tool to evaluate the role of the NR2B subunit in light input to the circadian system. In the present study, we sought to use ifenprodil to explore the role of NR2B subunits of the NMDA receptor in light-induced phase shifts of

Correspondence: Dr C. S. Colwell, as above.

E-mail: ccolwell@mednet.ucla.edu

*Present address: Department of Molecular Cell Biology, Leiden University Medical Center, PO Box 9600, 2300 RC Leiden, The Netherlands

†Present address: Department of Anatomy and Neurobiology, Morehouse School of Medicine, 720 Westview Drive, Atlanta, GA 30310, USA

Received 9 October 2007, revised 31 January 2008, accepted 11 February 2008

the circadian rhythm in wheel-running activity. Next, we examined the temporal patterns of NR2B subunit expression within SCN tissue. Finally, we examined the functional consequences of blocking the NR2B subunit on NMDA-evoked responses in individual SCN neurons.

Materials and methods

Animals

Adult male Syrian hamsters (*Mesocricetus auratus*) were purchased from Charles River Laboratories (arrived between 8 and 9 weeks of age). Hamsters were maintained on a 14/10 light/dark (LD) cycle and food and water were available *ad libitum*. They were housed individually in 20 × 40 × 20-cm Plexiglas cages equipped with 16-cm-diameter running wheels. Each revolution of the running wheel activated a microswitch on the outside of the cage. Switch activity was continuously monitored using VitalView software (Mini-Mitter, Sun River, OR, USA). All procedures complied with Public Health Service policies on the care and use of laboratory animals, and were approved by the Georgia State University institutional animal care and use committee.

Adult male C57Bl/6 mice were obtained from a breeding facility at University of California, Los Angeles. Mice were maintained on a daily LD (12/12) cycle for at least 10 days prior to the experiment. The time of lights-off in the colony rooms prior to the preparation of the brain slices was defined as zeitgeber time (ZT) 12 for the physiological analysis. It has been well established that cells in the SCN continue to show circadian oscillations when isolated from the animal in a brain slice preparation and that the phase of rhythm is dependent upon the LD cycle to which the mouse was exposed. All procedures complied with the Public Health Service policies on laboratory animal care and use, and were approved by the University of California, Los Angeles institutional animal care and use committee.

Surgery and microinjection procedures

At 7–10 days after their arrival, hamsters were anesthetized with sodium pentobarbital (90 mg/kg) and stereotaxically implanted with guide cannulae (26 ga, 11 mm) aimed at the SCN region (AP, +0.9 mm; ML, ±1.7 mm to bregma; angled 10° towards midline). Animals were housed in individual cages (20 × 20 × 40 cm) after surgery. Three days later cages were fitted with running wheels (16 cm diameter) and animals were allowed to entrain to LD 14/10. After entrainment had been verified, lights were disabled during the dark phase and remained off for the rest of the experiment.

At approximately 2 weeks after release into constant darkness, 200 nL of ifenprodil (Sigma, St Louis, MO, USA, no. I2892, 2 mg/mL in 10% dimethylsulfoxide) or vehicle (10% dimethylsulfoxide) was microinjected as a single bolus into the SCN region at circadian time (CT) 13.5 ($n = 13$) or CT 19 ($n = 13$). Activity onset was used to define CT 12 for these nocturnal organisms. Animals were returned to their home cages and immediately exposed to light (15 min, 150 lux). At approximately 3 weeks after the first microinjection (vehicle or drug)/light pulse, animals received a second microinjection (vehicle or drug)/light pulse. Thus, each animal received both a treatment of ifenprodil with light pulse and treatment of vehicle with light pulse at either CT 13.5 or CT 19. The injection order was randomly assigned.

At the completion of testing, animals received an overdose of sodium pentobarbital. India ink (50 nL) was delivered into the microinjection site via the guide cannula and brains were fixed in 10%

formalin. Sections (50 µm) were collected through the SCN and stained with cresyl violet. Injection sites were verified histologically using light microscopy. Only animals with sites within 500 µm of the SCN and not penetrating the third ventricle were included in the results.

Hamsters were gently restrained by hand during microinjection. Microinjections were delivered under dim red light (< 5 lux) with a 32-ga injection needle (Plastics One, Inc., Roanoke) attached by polyethylene tubing to a 1-µL Hamilton syringe (Hamilton Co., Reno). The 16-mm injection needle extended 5.2 mm beyond the guide cannula and 7.4 mm ventral to dura. The 200-nL volume was delivered over a 20-s interval and the needle was left in place for an additional 20 s before being slowly removed.

Circadian data collection and analysis

Running wheel data were collected, recorded and stored in 5-min bins by VitalView software and hardware (MiniMitter, Bend). Activity onset was defined as a minimum of 20 wheel revolutions in a 5-min bin for a minimum of three consecutive bins; the daily onset must follow the onset of the previous day by no less than 20 h. The circadian phase was estimated by fitting a regression line through the daily onsets of activity 7–10 days before and 7–10 days after the drug injection/light pulse. The first 3 days after treatment were excluded from the second regression to circumvent transient, unstable onsets. The magnitude of the phase shift was calculated by measuring the difference between the onsets of activity on the day of treatment predicted from the two regression estimates.

Brain slice preparation

Brain slices were prepared using standard techniques using mice between 4 and 6 weeks of age. Animals were anesthetized using isoflurane and killed by decapitation. Their brains were dissected and placed in cold oxygenated artificial cerebral spinal fluid (ACSF) containing (in mM): 130 NaCl, 26 NaHCO₃, 3 KCl, 5 MgCl₂, 1.25 NaH₂PO₄, 1.0 CaCl₂, 10 glucose (pH 7.2–7.4). After cutting slices (Microslicer, DSK model 1500E) from areas to be analysed, coronal sections were placed in ACSF (25–27 °C) for at least 1 h (in this solution CaCl₂ was increased to 2 mM and MgCl₂ was decreased to 2 mM). Slices were constantly oxygenated with 95% O₂/5% CO₂ (pH 7.2–7.4, osmolality 290–300 mOsm). This ACSF without MgCl₂ was used for recording NMDA-evoked responses.

RT-PCR

Brain slices containing SCN were prepared as described above. The SCN region was surgically separated from surrounding hypothalamic tissue under a dissecting microscope. Levels of NR2B mRNA were measured using semiquantitative real-time reverse transcription-polymerase chain reaction (RT-PCR). For each experiment, SCN tissue was collected from three mice at five time points (ZT 2, 6, 10, 16 and 23) and the RNA isolated via the Trizol method (Invitrogen, Carlsbad, CA, USA). The integrity and concentration of the RNA samples were analysed using an Agilent Bioanalyzer (microarray facility, University of California, Los Angeles). The RNA was determined to be of good quality by measuring 28S to 18S ribosomal peaks. Because of the very high sensitivity of the RT-PCR technique, several controls were run for both the harvesting of RNA and the RT-PCR reaction. First-strand cDNA synthesis of the extracted RNA was achieved with Oligo-dT primers and the ThermoScript RT-PCR system (Invitrogen). Primers

for the NR2B subunit were designed using Mfold (Michael Zuker, Rensselaer Polytechnic Institute) and Oligo6 (Molecular Biology Insights, Inc.) programs, producing amplification products between 80 and 110 bp. The polymerase chain reaction (PCR) was performed with each primer pair and samples run on an agarose gel to ensure appropriate product size. Specificity was confirmed by cloning into the pCRII vector (Invitrogen) and subsequently sequencing (UCLA sequencing facility). Semi-quantitative PCR with SYBR Green was performed using the iQ SYBR Green Supermix and the iCycler iQ Real-Time PCR machine (Bio-Rad, Hercules, CA, USA) to measure changes in the fluorescence signal. Analysis of melting curves showed only one peak in each sample, thus verifying that no other products were amplified. The cycle number at which the signals crossed a threshold set within the logarithmic phase were determined by the iCycler Q program (Bio-Rad). For the quantification of the results, we normalized cycle number values for *Nr2b* to beta-2 microglobulin (*B2m*). We have found that *B2m* shows no significant daily variation and thus is an appropriate control for these studies (unpublished observations). The efficiency of amplification of the primers was tested by serial dilutions of the RNA for both genes and cycle number against log(total RNA) was plotted. Standard curves for each primer pair were determined using a dilution series of a chosen SCN sample, from which cycle number was plotted against log. From this, the efficiency of the PCR was confirmed, relative starting quantities of the other unknown samples determined and expression values determined normalized to *B2m*.

Western blot analysis

Brain slices containing SCN were prepared as described above. The SCN region was surgically separated from surrounding hypothalamic tissue under a dissecting microscope. The tissue from three mice was pooled to form a single sample. The dissected tissue was then flash frozen in 500 μ L of ice-cold homogenization buffer (50 mM Tris-HCl, 50 mM NaF, 10 mM EGTA, 10 mM EDTA, 80 μ M sodium molybdate, 5 mM sodium pyrophosphate, 1 mM sodium orthovanadate, 0.01% Triton X-100, 4 mM para-nitrophenylphosphate). The homogenization buffer also contained cocktails of protease inhibitors (Protease Inhibitors Complete, Roche Molecular Biochemicals, Indianapolis, IN, USA) and protein phosphatase inhibitors (Protein Phosphatase Inhibitor Cocktail I and II, Sigma-Aldrich, St Louis, MO, USA). The tissue was homogenized with an ultrasonic cell disruptor (3×5 s). Immediately after homogenization, aliquots were removed for protein analysis and equal amounts of denaturing protein loading buffer [0.5 M Tris-HCl, pH 6.8, 4.4% (w/v) sodium dodecyl sulfate, 20% (v/v) glycerol, 2% 2-mercaptoethanol, bromophenol blue] were added. These homogenates were kept on ice for ~ 45 min while protein concentrations were determined using a protein assay kit (Bio-Rad). Homogenates containing 20–30 μ g of protein each were electrophoresed on 15% sodium dodecyl sulfate–polyacrylamide gel electrophoresis gels, transferred to nitrocellulose membranes and probed with rabbit polyclonal antibodies (Chemicon, Temecula, CA, USA) against phospho-NR2B (ser 1303; 1 : 1000) and total NR2B (1 : 1000). The membranes were incubated with horseradish peroxidase-conjugated anti-rabbit secondary IgG (1 : 1000) and protein signals were visualized with chemiluminescence (Immun-Star HRP detection kit, Bio-Rad). A phospho-imager was used for quantification and day/night comparisons were analysed simultaneously, using identical settings. Protein bands were boxed and the integrated intensity of all of the pixels within that band was calculated above the object average background levels of boxes of the same size. Percent

changes attributable to temporal variation were calculated relative to the optical density volume of the corresponding untreated protein bands within a single experiment.

Whole-cell patch-clamp electrophysiology

Methods were similar to those described previously (Colwell, 2001; Michel *et al.*, 2002). Electrodes were pulled on a multistage puller (Sutter P-97, Novato, CA, USA). Electrode resistance in the bath was typically 4–6 M Ω . The standard solution in the patch pipette contained (in mM): 125 Cs-methanesulfonate, 8 Hepes, 5 MgATP, 4 NaCl, 3 KCl, 1 MgCl₂, 1 GTP, 0.1 leupeptin and 10 phosphocreatine. The pH was adjusted to 7.25–7.3 using CsOH and the osmolarity to 280–290 mOsm using sucrose. The measurement of NMDA currents was conducted in extracellular solution that contained no external Mg²⁺. Whole-cell recordings were obtained with a 200B amplifier and monitored on-line with pCLAMP (both from Axon Instruments, Foster City, CA, USA). To minimize changes in offset potentials with changing ionic conditions, the ground path used an ACSF agar bridge. Cells were approached with slight positive pressure (2–3 cm H₂O) and offset potentials were corrected. The liquid junction potential was –14 mV but values shown in the figures and text were not corrected for this value. The pipette was lowered to the vicinity of the membrane while maintaining positive pressure. After forming a high-resistance seal (2–10 G Ω) by applying negative pressure, a second pulse of negative pressure was used to break the membrane. While entering the whole-cell mode, a repetitive test pulse of 10 mV was delivered in a passive potential range (approximately –60 to –70 mV). Whole-cell capacitance and electrode resistance were neutralized and compensated (50–80%) using the test pulse. Data acquisition was then initiated. Series and input resistance was monitored repeatedly by checking the response to small pulses in a passive potential range. Series resistance was not compensated and the maximal voltage error due to this resistance was calculated to be 6 mV. The access resistance of these cells ranged from 20 to 40 M Ω , whereas the cell capacitance was typically between 6 and 18 pF.

Under voltage clamp ($V_m = -70$ mV), the holding current was monitored throughout the experiment. In addition, the neuron's current–voltage relationship was measured every 2–3 min by moving the cell's membrane potential through a series of voltage steps. In these experiments, after the initial control voltage steps (no drug), each cell was exposed to NMDA followed by a wash until the response returned to baseline. Current measurements were normalized to cell size by dividing peak inward current by cell capacitance.

Ca²⁺ imaging

Methods were similar to those described previously (Colwell, 2000, 2001). In brief, a cooled charge-coupled device camera (Microview model, 1317 \times 1035-pixel format, Princeton Instruments, Monmouth Junction, NJ, USA) was added to the Olympus fixed stage microscope to measure fluorescence. In order to load the Ca²⁺ indicator dye into cells, slices were incubated with membrane-permeable fura2 AM (50 μ M) at 37 $^{\circ}$ C for 10 min. The fluorescence of fura2 was excited alternately at wavelengths of 357 and 380 nm by means of a high-speed wavelength-switching device (Sutter, Lambda DG-4). Image analysis software (MetaFluor, Universal Imaging, Downingtown, PA, USA) allowed the selection of several regions of interest within the field from which measurements were taken. In order to minimize bleaching, the intensity of excitation light and sampling frequency were kept as low as possible.

Drug application

For most of the acute electrophysiology and Ca^{2+} imaging experiments, solution exchanges within the slice were achieved by a rapid gravity-feed delivery system utilizing an electronically controlled valve. Whereas the time required for the valve to switch is measured in milliseconds, the time required for the solution to reach the cell is much more sluggish. We have used dyes to measure the time required for solution exchange and estimate that it takes about 60 s for the drug to reach the neuron and about 90 s for a full exchange of the experimental and control solutions. In these experiments, NMDA was applied for 120 s with maximal responses typically observed approximately 90 s after start of treatment. I/V curves were measured before, during and after NMDA treatment. In the cases in which multiple NMDA treatments were applied to a neuron, there was at least a 5-min interval between treatments to allow the neuron to recover. Ifenprodil was applied for 240 s and, in some cases, these treatments were immediately (< 1 s) followed by application of NMDA. Using this method of drug application, some ifenprodil will have rinsed off during NMDA application and it is possible that we are underestimating the magnitude of the inhibitory effects. However, our data indicate that the inhibitory effects of ifenprodil are long lasting and only wash out after 10–15 min. We feel that this under-estimation would be minimal. For a few of the experiments, NMDA was applied via a fast perfusion system (ALA Scientific Instruments, Westbury, New York, USA). With this system, the NMDA reaches the neuron very quickly (< 1 s). In all cases, the drugs were mixed into zero Mg^{2+} ACSF. Chemicals were purchased from Sigma.

Statistical analyses

Group differences were evaluated using *t*-tests or one-way ANOVA followed by Tukey test for pairwise comparisons. Values were considered significantly different if $P < 0.05$. These tests were performed using SigmaStat (Systat, Point Richmond, CA, USA). In the text, values are shown as mean \pm SEM.

Results

Light-induced phase shifts of the circadian system are dependent on NR2B subunits of the NMDA receptor

The wheel-running activity of hamsters in constant darkness was measured. Exposure to light (15 min) at CT 13.5 resulted in significantly smaller phase delays when immediately preceded by a microinjection (200 nL) of ifenprodil (2 mg/mL) into the SCN region than when preceded by a microinjection of vehicle into the SCN region (*t*-test, $P = 0.002$; Fig. 1). Exposure to light (15 min) at CT 19 resulted in significantly smaller phase advances when immediately preceded by a microinjection of ifenprodil into the SCN region than when preceded by a microinjection of vehicle (*t*-test, $P = 0.032$; Fig. 1). Neither ifenprodil nor vehicle alone caused significant phase shifts by themselves at either phase (Fig. 1). Examples of the wheel-running activity records for each of the groups are shown in Fig. 2.

Transcripts of the NR2B subunit vary with time of day in SCN tissue

In the next set of experiments, we examined the possibility that the relative expression of the NR2B subunit varies with time of day in the mouse SCN. We tested for differences in the mRNA levels for the NR2B subunit using semiquantitative real-time PCR. SCN tissue was

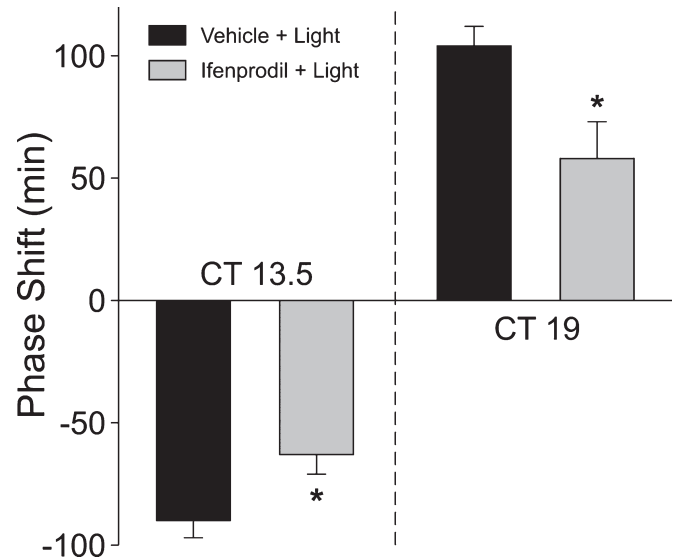


FIG. 1. Microinjection of ifenprodil inhibits the magnitude of light-induced phase shifts in the circadian rhythm in wheel-running activity. Histograms plot the mean phase shift of hamsters in constant darkness that received a treatment of either vehicle (200 nL) plus light or ifenprodil (200 nL, 2 mg/mL) plus light. Other groups included hamsters treated with vehicle or ifenprodil alone. Light treatments (15 min, 150 lux) were delivered at either CT 13.5 or CT 19. The vehicle or drug treatments were delivered immediately prior to light. The placement of the cannula into the SCN region was histologically confirmed. $N = 6$ –8 for all points; error bars represent SEM. Values were analysed with *t*-test; *significance at $P < 0.05$.

collected from 15 mice at five time points (ZT 2, 6, 10, 16 and 23) and SCN from three mice pooled for each sample. The expression of the NR2B subunit was normalized to a housekeeping gene (*B2m*), which has minimal daily variation (unpublished observations). The experiment was repeated three times and the results are shown in Fig. 3. There was a clear daily variation in the expression of the NR2B subunit (ANOVA; $P < 0.001$), with peak expression averaging 335% higher than the trough.

Levels of the phospho-NR2B subunit protein vary with time of day in SCN tissue

In order to explore possible rhythmic expression of protein levels, western blotting was performed on homogenates of SCN. SCN tissue collected during the day (ZT 6) was compared with SCN tissue collected during the early night (ZT 16) and late night (ZT 23) with protein from the SCN of three mice pooled for each sample. An antibody against tubulin was used as a loading control. The experiment was repeated three times and the results are shown in Fig. 4. Western blotting with a polyclonal antibody raised against the C-terminus of mouse NR2B gave a clear band at the expected molecular weight (180 kDa). This 180-kDa band was lost upon pre-incubation of the NR2B primary antibody with a control peptide (data not shown). Although the NR2B protein was expressed in SCN tissue, there were no significant differences between the times sampled (Fig. 4B). Western blotting with a polyclonal antibody raised against human phospho-NR2B (ser 1303) also gave a clear band at the expected molecular weight (~ 180 kDa). This 180-kDa band was lost upon pre-incubation of the primary antibody with a control peptide (data not shown). The expression of the phospho-NR2B (ser 1303) in SCN tissue varied with the time of day (ANOVA; $P < 0.05$) in each of

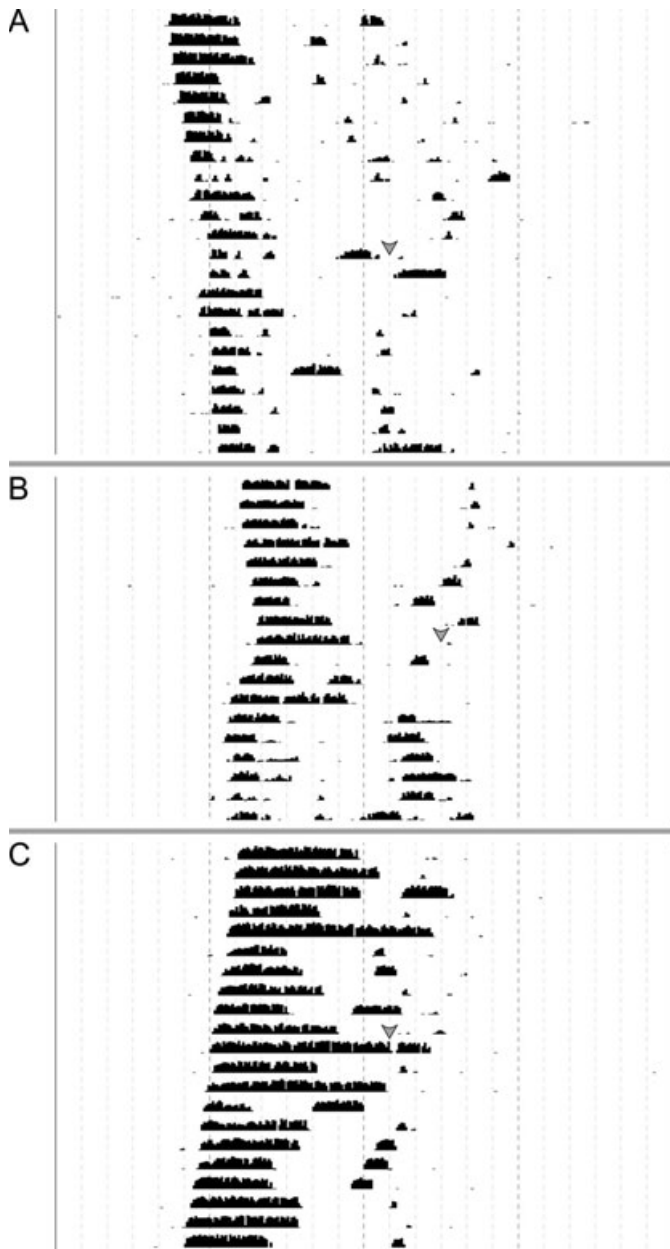


FIG. 2. Locomotor activity records from experimental and control animals maintained in constant darkness. Each horizontal line represents the activity record for a 24-h day and successive days are plotted from top to bottom. Grey arrows represent the time of light and/or drug treatment. (A) Activity record illustrating the inhibition of the phase-advancing effects of light by an intra-SCN injection of ifenprodil at CT 19. (B) Activity record illustrating light-induced phase shift of locomotor activity. Hamsters were exposed to light at CT 19 with vehicle delivered immediately prior to light. (C) Activity record illustrating the lack of effect of an injection of ifenprodil at CT 19 on the phase of the circadian rhythm in locomotor activity.

three experiments, with peak expression on average 267% higher than the trough (Fig. 4B).

Ifenprodil inhibits the magnitude of NMDA currents in SCN neurons

To test the hypothesis that NR2B subunits contribute to the post-synaptic response of SCN neurons to NMDA stimulation, whole-cell patch-clamp recording techniques were used to measure currents

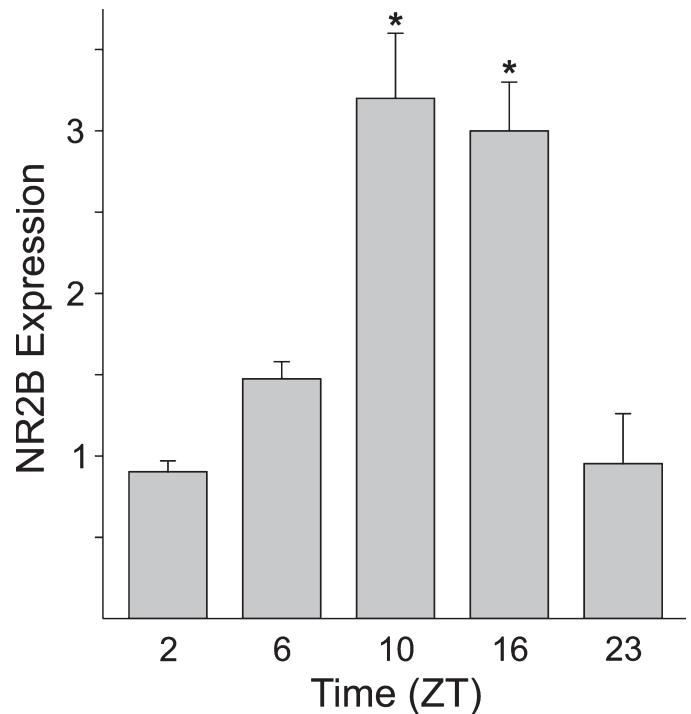


FIG. 3. NR2B transcripts are rhythmically expressed in SCN tissue. Semi-quantitative RT-PCR was used to measure levels of the transcript. The values shown are determined by a standard curve and normalized to the housekeeping gene beta-2 microglobulin. The histogram plots the mean results of three independent experiments with error bars representing SEM. For each experiment, SCN tissue was collected from 15 mice at five time points (ZT 2, 6, 10, 16 and 23) with mRNA from each time point pooled from three mice. Values were analysed with ANOVA followed by Tukey test for pairwise comparisons. *Significance at $P < 0.05$ compared with sample at ZT 2.

evoked by NMDA in ventral SCN neurons during the night. As the RHT input to the mouse SCN is focused in the ventral SCN region, we focused our recording in this region of the SCN. These measurements of NMDA currents were conducted in extracellular solution that contained no external Mg^{2+} to decrease the voltage dependence of this current. For the first set of experiments, the voltage dependence of the NMDA-evoked currents was measured by moving the neuron through a series of voltage steps (from -120 to 40 mV) before, during and after treatment with NMDA in the bath. NMDA currents were blocked by the competitive receptor antagonist 2-amino-5-phosphonovaleate ($50 \mu M$, 240 s) and were stable over 20 min (data not shown, $n = 8$). The bath application of NMDA ($25 \mu M$, 120 s) produced a normalized peak inward current of -6.2 ± 0.9 pA/pF ($n = 16$). Treatment with ifenprodil ($3 \mu M$, 240 s) significantly reduced the magnitude of NMDA-evoked currents in the SCN neurons examined ($47 \pm 5\%$ decrease in peak current in responding neurons; 16/16 neurons responded; t -test, $P < 0.001$; Fig. 5A). In most neurons, the magnitude of the NMDA current recovered to pre-treatment values after a 15-min wash. The inhibitory effects of ifenprodil were concentration dependent with $0.1 \mu M$ producing no inhibition ($1 \pm 4\%$, $n = 5$) and $1.0 \mu M$ producing a measurable decrease ($24 \pm 4\%$, $n = 5$; $P = 0.05$) in the magnitude of the peak NMDA current. Bath application of exogenous zinc ($10 \mu M$, 240 s) produced a modest reduction in the magnitude of the peak NMDA current ($19 \pm 3\%$, $n = 6$, t -test, $P = 0.05$). Finally, we examined the effects of ifenprodil on the currents evoked by the fast, focal application of NMDA ($100 \mu M$) on ventral SCN neurons held at -70 mV (Fig. 5B). Under these conditions, NMDA produced a peak inward current of

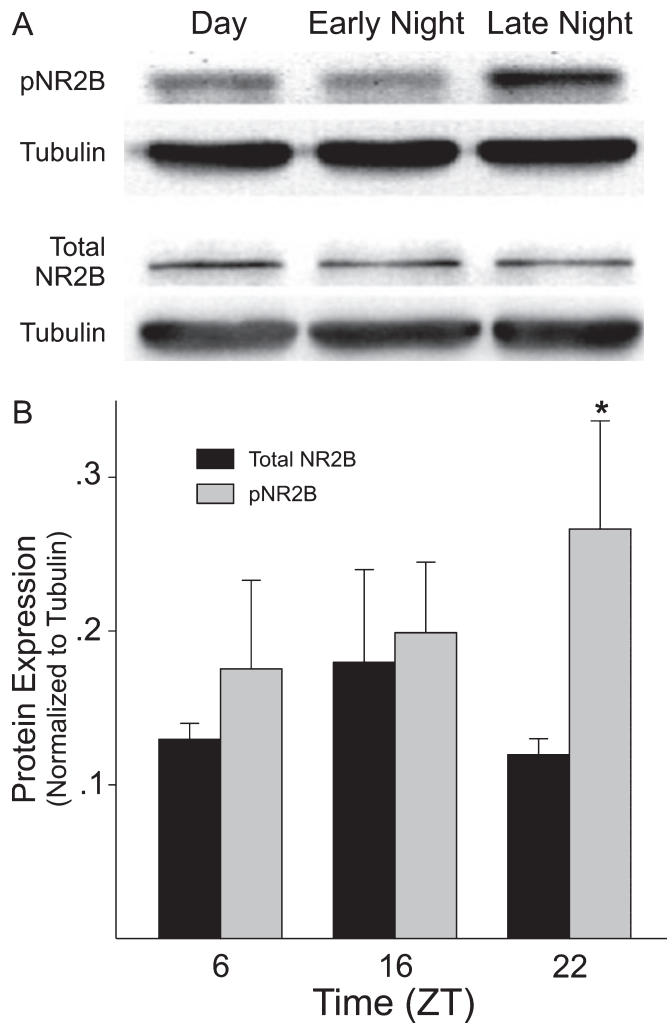


FIG. 4. Phospho-NR2B levels vary with time of day in SCN tissue. Western blots were used to measure levels of phospho-NR2B and total NR2B. (A) Top panels show examples of the blots. (B) Histograms plot the mean results of three independent experiments with error bars representing SEM. Values are shown normalized to tubulin. For each experiment, SCN tissue was collected from mice at three time points (ZT 6, 16 and 22) with protein extracts from each time point pooled from three mice. Values were analysed with ANOVA followed by Tukey test for pairwise comparisons. *Significance at $P < 0.05$ compared with sample at ZT 6.

-4.75 ± 0.7 pA/pF ($n = 9$) and application of ifenprodil caused a significant reduction in the magnitude of this current ($68 \pm 6\%$, $n = 9$; t -test, $P < 0.01$). The application of the control solution or ifenprodil by itself did not evoke a change in the holding current (data not shown). Together, these data indicate that the NR2B subunit makes a significant contribution to NMDA-evoked currents in the ventral SCN.

NR2B subunit contributes to the NMDA-evoked Ca^{2+} influx in SCN neurons

In order to test the hypothesis that the NR2B subunit contributes to NMDA-induced Ca^{2+} transients in ventral SCN neurons during the night (ZT 15–17), a bulk loading procedure was used to load cells with a membrane-permeable form of the Ca^{2+} indicator dye fura2. Cells that exhibited uneven loading due to dye sequestration were not included in the data set. Small cell types including glia were easily identified and were also excluded from the data set. These measurements of

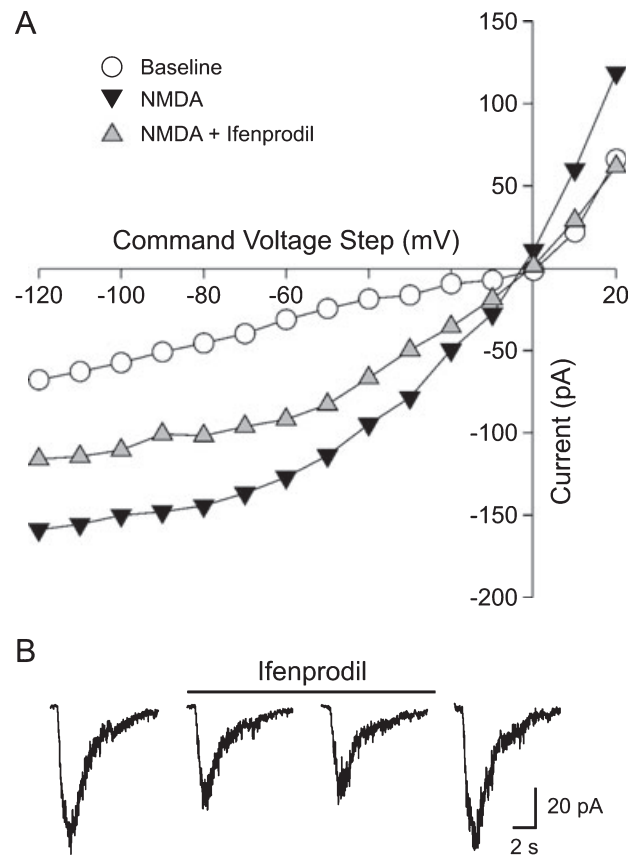


FIG. 5. Ifenprodil inhibits the magnitude of NMDA-evoked currents in SCN neurons. Whole-cell patch-clamp recording methods were used to measure NMDA currents in ventral SCN during the night in a zero Mg^{2+} solution. (A) The current–voltage relationship of SCN neuron under baseline, NMDA ($25 \mu M$) and NMDA plus ifenprodil ($3 \mu M$). In this example, the drugs were applied in the bath and the neuron moved to a series of voltage steps. (B) The inhibitory effects of ifenprodil ($3 \mu M$) on the inward current generated in response to the focal application of NMDA ($100 \mu M$). The neuron was held at -70 mV during this recording.

NMDA-evoked responses were carried out in an extracellular solution that contained no Mg^{2+} . The bath application of NMDA ($25 \mu M$, 60 s) produced a peak Ca^{2+} increase of 56 ± 4 nM ($n = 44$) measured in the soma. Treatment with ifenprodil alone ($3 \mu M$, 240 s) did not cause a significant change in basal Ca^{2+} levels in SCN cells. After treatment with ifenprodil, the magnitude of the NMDA-induced Ca^{2+} transient was significantly reduced (t -test, $P < 0.05$) with an average NMDA response of 35 ± 4 nM ($n = 44$). The imaging data indicate that the NR2B subunit makes a significant contribution to NMDA-evoked Ca^{2+} responses in the ventral SCN.

Discussion

The data presented in this study indicate that the NR2B subunit of the NMDA receptor is an important component of the light input to the circadian system. Behaviorally, the localized injection of the NR2B antagonist ifenprodil significantly reduced the magnitude of the light response as measured by wheel-running behavior. Hamsters were used for these initial behavioral studies due to the precision of their wheel-running activity and the depth of background information using this species for studies of the photic regulation of the circadian system (e.g. Morin & Allen, 2006). Both the NR2B transcript (O'Hara *et al.*, 1995; Moriya *et al.*, 2000) and protein are present in SCN tissue. Finally,

ifenprodil significantly reduced the magnitude of both NMDA currents and NMDA-evoked Ca^{2+} influx recorded at the level of single SCN neurons. At either the behavioral or cellular analysis, the blockade of the NR2B subunits reduced but did not eliminate the responses. This fits with our understanding of the NMDA receptor as a multimeric structure of which the NR2B subunit would be just one component. At each level of analysis, ifenprodil caused an approximate 40–60% reduction in the magnitude of the response. Ifenprodil has been widely used as a blocker of NMDA receptors containing the NR2B subunit (Williams, 1993, 2001; Neyton & Paoletti, 2006). Ifenprodil antagonizes NR1/NR2B receptors with greater than 200-fold preference compared with NR1/NR2A receptors. This antagonist is also voltage independent so it can be applied under the resting membrane potentials used in the present study. However, like any pharmacological agent, there are limitations that should be considered in the interpretation of the present data (see Neyton & Paoletti, 2006). For example, at the concentration used (1–3 μM), ifenprodil does not fully antagonize responses mediated by NR1/NR2B receptors. In addition, ifenprodil does not discriminate between NR1/NR2B and triheteromeric NR1/NR2A/NR2B receptors. The latter may well be present in the SCN as the NR2A subunit is expressed in the SCN (O'Hara *et al.*, 1995). Furthermore, the NMDA-evoked currents were modestly inhibited by exogenous zinc and this ion displays strong selectivity for NR2A-containing receptors (Rachline *et al.*, 2005). Our data do not allow us to differentiate between a mixed population of NR1/NR2B and NR1/NR2A receptors or triheteromeric NMDA receptors containing NR1/NR2A/NR2B subunits. The present data do indicate that the NR2B subunit is an important contributor to the post-synaptic response of SCN neurons to retinal input.

The expression of the NR2B subunit and its phosphorylation state vary as a function of time of day within SCN neurons. Under LD conditions, we found significant time-of-day variation in the NR2B message as measured by RT-PCR as well as in the levels of phosphorylated protein. There are a number of cases in which the contributions of the subunits that make up the NMDA receptor are actively regulated in a way that leads to changes in their functional properties. For example, developmentally immature neurons tend to express more of the NR2B subunit and, as a result, exhibit NMDA currents with slower kinetics and more sensitivity to the NR2B blocker ifenprodil (Loftis & Janowsky, 2003; Lopez de Armentia & Sah, 2003). As neurons mature, the expression of the NR2B subunit typically decreases relative to the NR2A subunit and drives changes in the functional properties of these receptors. In some cases, switches in subunit composition can occur quite rapidly. For example, NMDA receptors in the visual cortex of dark-reared animals that were exposed to light exhibited a rapid (within 1 h) switch in subunit composition from NR2B to NR2A (Quinlan *et al.*, 1999). Post-translational events can also regulate NMDA currents through phosphorylation of the receptor subunit. In one of the best-studied examples, brain-derived neurotrophic factor enhanced the NMDA-evoked response in the hippocampus through selective phosphorylation of the NR2B subunit (Lin *et al.*, 1998; Levine & Kolb, 2000). In the SCN, brain-derived neurotrophic factor also enhances the NMDA component of the evoked synaptic response through a mechanism blocked by ifenprodil (Kim *et al.*, 2006). Thus, in the SCN, nightly changes in NR2B phosphorylation could result in a rhythmic change in the functional properties of the NMDA receptor.

Diurnal changes in the NMDA receptors localized within the SCN would be functionally important to the circadian system. There is a variety of evidence that the NMDA receptor plays a critical role in mediating photic regulation of the circadian system (Morin & Allen, 2006). Anatomical studies report that identified RHT terminals

innervating the SCN show glutamate immunoreactivity associated with synaptic vesicles (Castel *et al.*, 1993; Chen & Pourcho, 1995) and NMDA receptors (GluR) are present in the SCN (Gannon & Rea, 1993, 1994; Mikkelsen *et al.*, 1993; Ishida *et al.*, 1994; O'Hara *et al.*, 1995). NR2B transcripts are present in the SCN (O'Hara *et al.*, 1995; Moriya *et al.*, 2000; Matsushita *et al.*, 2006). Electrophysiologically, most SCN neurons are excited by application of NMDA, and NMDA receptors contribute to the excitatory post-synaptic potentials recorded in the SCN (Kim & Dudek, 1991; Jiang *et al.*, 1997; Colwell, 2001). Functionally, application of NMDA causes phase shifts in the circadian rhythm of neural activity recorded from the SCN *in vitro* (Shibata *et al.*, 1994; Ding *et al.*, 1994) or *in vivo* (Mintz *et al.*, 1999). Finally, NMDA receptor antagonists block light-induced phase shifts and fos induction in the SCN *in vivo* (Colwell & Menaker, 1992; Abe & Rusak, 1994).

One of the fundamental features of circadian oscillators is that their response to environmental stimulation varies depending on the phase of the daily cycle when the stimuli are applied (Roenneberg *et al.*, 2003). For example, a light treatment, which can produce phase shifts of the oscillator when applied during the subjective night, has no effect when applied during the subjective day. In fact, this periodic sensitivity to photic stimulation is a central feature of current models of entrainment, i.e. the process by which circadian oscillators are synchronized to the environment. Despite its importance, the cellular and molecular mechanisms behind this differential sensitivity are still not known. There is clear evidence that this 'diurnal gating' occurs at the level of SCN neurons. Two studies have shown that electrical stimulation of the RHT causes the same daily pattern of light-like phase shifts of the circadian system both *in vivo* (de Vries *et al.*, 1994) and *in vitro* (Shibata & Moore, 1993), i.e. phase shifts occur during the night but not during the day. In addition, application of NMDA causes light-like phase shifts of the circadian rhythm in neuronal activity in the SCN *in vitro* (Ding *et al.*, 1994; Shibata *et al.*, 1994). Our previous work has demonstrated that the circadian system gates the magnitude of NMDA-induced currents and Ca^{2+} transients (Colwell, 2001). These responses were larger in the night, when light causes phase shifts, than during the day, when light is without effect. Additional support comes from the work of Pennartz *et al.* (2001) who found that the NMDA component of the evoked excitatory response is larger in the night than in the day. Part of the gating mechanism determining the magnitude of the response to light appears to occur at the level of NMDA receptors in SCN neurons. Therefore, based on our experimental observation, we propose that the daily rhythm in contribution of the NR2B subunit is responsible for the daily rhythms in NMDA-evoked responses in the SCN. One puzzle that will need to be examined in future experiments is understanding why the phosphorylation of the NR2B subunit peaks in late night and how this may relate to the function of the NMDA receptor-driven signaling cascades.

Many unanswered questions remain as to how the circadian oscillators in the SCN respond to activation of amino-methyl propionic acid and NMDA receptors. In the simplest case, light causes the release of glutamate. The post-synaptic amino-methyl propionic acid receptors are responsible for the initial depolarization of the post-synaptic membrane. This depolarization is required before the neuron's membrane potential moves into the voltage range at which the NMDA receptors become activated. So what are the next steps in the signal transduction cascade? The concentration of intracellular Ca^{2+} in neurons is tightly controlled by a variety of known channels, pumps and buffers. Activation of NMDA receptors causes an increase in Ca^{2+} directly by opening ion channels permeable to Ca^{2+} and indirectly through activation of voltage-sensitive Ca^{2+}

channels and Ca²⁺-induced Ca²⁺ release from intracellular stores. The relative contribution of these three Ca²⁺ sources to the NMDA-induced Ca²⁺ transients in SCN neurons is not yet known. Kim *et al.* (2005) have evidence indicating that voltage-sensitive Ca²⁺ currents are required for glutamate-induced phase shifts of rat SCN neural activity rhythm. In addition, ryanodine receptors may mediate light- and glutamate-induced phase delays of the circadian system (Ding *et al.*, 1997) as well as regulate the electrical activity of SCN neurons (Aguilar-Roblero *et al.*, 2007). Similarly, earlier work also indicates that a Ca²⁺ influx is required for light regulation of the circadian oscillator found in the retinas of marine mollusks (McMahon & Block, 1987; Khalsa *et al.*, 1993; Colwell *et al.*, 1994) and more recently in mammals (Lundkvist *et al.*, 2005). Thus, the NMDA receptor-mediated Ca²⁺ influx is likely to be a major transducer of light information to the circadian system.

The signal transduction events following the influx of Ca²⁺ are beginning to be understood and seem to include a number of signaling pathways (Cermakian & Sassone-Corsi, 2002; Gillette & Mitchell, 2002; Meijer & Schwartz, 2003). Although the roles of each pathway are not yet clear, strong evidence exists for the importance of the release of nitric oxide, activation of the Ras/MAP kinase cascade and phosphorylation of the cAMP-responsive element binding protein (Ding *et al.*, 1994; Obrietan *et al.*, 1998; Gau *et al.*, 2002; Travnickova-Bendova *et al.*, 2002; Tischkau *et al.*, 2003). Within the cell's nucleus, activation of these signal transduction pathways ultimately results in chromatin modifications, activation of immediate early genes and transcriptional regulation of *mPer1* and *mPer2* (Kornhauser *et al.*, 1996; Yan *et al.*, 1999; Crosio *et al.*, 2000; Miyake *et al.*, 2000; Gau *et al.*, 2002; Tischkau *et al.*, 2003). In many cell types, these processes are all strongly Ca²⁺ dependent (Bito *et al.*, 1997; West *et al.*, 2001). Thus, the NR2B subunit, through its modulation of NMDA-evoked Ca²⁺ transients, is likely to play a pivotal role in linking membrane events to changes in gene expression relevant to the circadian timing system.

Acknowledgements

D.L.H., J.C.E. and H.E.A. provided the behavioral analysis, D.S. and D.L. provided the RT-PCR measurements, L.M.W. was responsible for the western blots, A.S. was responsible for the optical imaging data, and J.H.H. and K.L. were responsible for the measurements of the NMDA currents. Supported by NIH MH58789 to H.E.A. and NS 043169 to C.S.C.

Abbreviations

ACSF, artificial cerebral spinal fluid; CT, circadian time; LD, light/dark; NMDA, N-methyl-D-aspartate; PCR, polymerase chain reaction; RHT, retino-hypothalamic tract; RT-PCR, reverse transcription-polymerase chain reaction; SCN, suprachiasmatic nucleus; ZT, zeitgeber time.

References

- Abe, H. & Rusak, B. (1994) Physiological mechanisms regulating photic induction of Fos-like protein in hamster suprachiasmatic nucleus. *Neurosci. Biobehav. Rev.*, **18**, 531–536.
- Aguilar-Roblero, R., Mercado, C., Alamilla, J., Laville, A. & Diaz-Muñoz, M. (2007) Ryanodine receptor Ca²⁺-release channels are an output pathway for the circadian clock in the rat suprachiasmatic nuclei. *Eur. J. Neurosci.*, **26**, 575–582.
- Berson, D.M. (2003) Strange vision: ganglion cells as circadian photoreceptors. *Trends Neurosci.*, **26**, 314–320.
- Bito, H., Deisseroth, K. & Tsien, R.W. (1997) Ca²⁺-dependent regulation in neuronal gene expression. *Curr. Opin. Neurobiol.*, **7**, 419–429.
- Castel, M., Belenky, M., Cohen, S., Ottersen, O.P. & Storm-Mathisen, J. (1993) Glutamate-like immunoreactivity in retinal terminals of the mouse suprachiasmatic nucleus. *Eur. J. Neurosci.*, **5**, 368–381.
- Cermakian, N. & Sassone-Corsi, P. (2002) Environmental stimulus perception and control of circadian clocks. *Curr. Opin. Neurobiol.*, **12**, 359–365.
- Chen, B. & Pourcho, R.G. (1995) Morphological diversity and glutamate immunoreactivity of retinal terminals in the suprachiasmatic nucleus of the cat. *J. Comp. Neurol.*, **361**, 108–118.
- Colwell, C.S. (2000) Circadian modulation of calcium levels in cells in the suprachiasmatic nucleus. *Eur. J. Neurosci.*, **12**, 571–576.
- Colwell, C.S. (2001) NMDA-evoked calcium transients and currents in the suprachiasmatic nucleus: Gating by the circadian system. *Eur. J. Neurosci.*, **13**, 1420–1428.
- Colwell, C.S. & Menaker, M. (1992) NMDA as well as non-NMDA receptor antagonists can prevent the phase-shifting effects of light on the circadian system of the golden hamster. *J. Biol. Rhythms*, **7**, 125–136.
- Colwell, C.S., Whitmore, D., Michel, S. & Block, G.D. (1994) Calcium plays a central role in phase shifting the ocular circadian pacemaker of *Aplysia*. *J. Comp. Physiol.*, **175**, 415–423.
- Crosio, C., Cermakian, N., Allis, C.D. & Sassone-Corsi, P. (2000) Light induces chromatin modification in cells of the mammalian circadian clock. *Nat. Neurosci.*, **3**, 1241–1247.
- Cull-Candy, S., Brickley, S. & Farrant, M. (2001) NMDA receptor subunits: diversity, development and disease. *Curr. Opin. Neurobiol.*, **11**, 327–335.
- Ding, J.M., Chen, D., Weber, E.T., Faiman, L.E., Rea, M.A. & Gillette, M.U. (1994) Resetting the biological clock: Mediation of nocturnal circadian shifts by glutamate and NO. *Science*, **266**, 1713–1717.
- Ding, J.M., Faiman, L.E., Hurst, W.J., Kuriashkina, L.R. & Gillette, M.U. (1997) Resetting the biological clock: mediation of nocturnal CREB phosphorylation via light, glutamate, and nitric oxide. *J. Neurosci.*, **17**, 667–675.
- Gannon, R.L. & Rea, M.A. (1993) Glutamate receptor immunoreactivity in the rat suprachiasmatic nucleus. *Brain Res.*, **622**, 337–342.
- Gannon, R.L. & Rea, M.A. (1994) In situ hybridization of antisense mRNA oligonucleotides for AMPA, NMDA and metabotropic glutamate receptor subtypes in the rat suprachiasmatic nucleus at different phases of the circadian cycle. *Brain Res. Mol. Brain Res.*, **23**, 338–344.
- Gau, D., Lemberger, T., von Gall, C., Kretz, O., Le Minh, N., Gass, P., Schmid, W., Schibler, U., Korf, H.W. & Schuetz, G. (2002) Phosphorylation of CREB Ser142 regulates light-induced phase shifts of the circadian clock. *Neuron*, **34**, 245–253.
- Gillette, M.U. & Mitchell, J.W. (2002) Signaling in the suprachiasmatic nucleus: selectively responsive and integrative. *Cell Tissue Res.*, **309**, 99–107.
- Hastings, M.H. & Herzog, E.D. (2004) Clock genes, oscillators, and cellular networks in the suprachiasmatic nuclei. *J. Biol. Rhythms*, **19**, 400–413.
- Ishida, N., Matsui, M., Mitsui, Y. & Mishina, M. (1994) Circadian expression of NMDA receptor mRNAs, epsilon 3 and zeta 1, in the suprachiasmatic nucleus of rat brain. *Neurosci. Lett.*, **166**, 211–215.
- Jiang, Z.G., Yang, Y., Liu, Z.P. & Allen, C.N. (1997) Membrane properties and synaptic inputs of suprachiasmatic nucleus neurons in rat brain slices. *J. Physiol.*, **499**, 141–159.
- Khalsa, S.B., Ralph, M.R. & Block, G.D. (1993) The role of extracellular calcium in generating and in phase-shifting the *Bulla* ocular circadian rhythm. *J. Biol. Rhythms*, **8**, 125–139.
- Kim, Y.I. & Dudek, F.E. (1991) Intracellular electrophysiological study of suprachiasmatic nucleus neurons in rodents: excitatory synaptic mechanisms. *J. Physiol.*, **444**, 269–287.
- Kim, D.Y., Choi, H.J., Kim, J.S., Kim, Y.S., Jeong, D.U., Shin, H.C., Kim, M.J., Han, H.C., Hong, S.K. & Kim, Y.I. (2005) Voltage-gated calcium channels play crucial roles in the glutamate-induced phase shifts of the rat suprachiasmatic circadian clock. *Eur. J. Neurosci.*, **21**, 1215–1222.
- Kim, Y.I., Choi, H.J. & Colwell, C.S. (2006) Brain-derived neurotrophic factor regulation of N-methyl-D-aspartate receptor-mediated synaptic currents in suprachiasmatic nucleus neurons. *J. Neurosci. Res.*, **84**, 1512–1520.
- Kornhauser, J.M., Mayo, K.E. & Takahashi, J.S. (1996) Light, immediate-early genes, and circadian rhythms. *Behav. Genet.*, **26**, 221–240.
- Levine, E.S. & Kolb, J.E. (2000) Brain-derived neurotrophic factor increases activity of NR2B-containing N-methyl-D-aspartate receptors in excised patches from hippocampal neurons. *J. Neurosci. Res.*, **62**, 357–362.
- Lin, S.Y., Wu, K., Levine, E.S., Mount, H.T., Suen, P.C. & Black, I.B. (1998) BDNF acutely increases tyrosine phosphorylation of the NMDA receptor subunit 2B in cortical and hippocampal postsynaptic densities. *Brain Res. Mol. Brain Res.*, **55**, 20–27.
- Lofis, J.M. & Janowsky, A. (2003) The N-methyl-D-aspartate receptor subunit NR2B: localization, functional properties, regulation, and clinical implications. *Pharmacol. Ther.*, **97**, 55–85.

- Lopez de Armentia, M. & Sah, P. (2003) Development and subunit composition of synaptic NMDA receptors in the amygdala: NR2B synapses in the adult central amygdala. *J. Neurosci.*, **23**, 6876–6883.
- Lundkvist, G.B., Kwak, Y., Davis, E.K., Tei, H. & Block, G.D. (2005) A calcium flux is required for circadian rhythm generation in mammalian pacemaker neurons. *J. Neurosci.*, **25**, 7682–7686.
- Matsushita, T., Amagai, Y., Terai, K., Kojima, T., Obinata, M. & Hashimoto, S. (2006) A novel neuronal cell line derived from the ventrolateral region of the suprachiasmatic nucleus. *Neuroscience*, **140**, 849–856.
- McBain, C.J. & Mayer, M.L. (1994) N-methyl-D-aspartic acid receptor structure and function. *Physiol. Rev.*, **74**, 723–760.
- McMahon, D.G. & Block, G.D. (1987) The Bulla ocular circadian pacemaker. I. Pacemaker neuron membrane potential controls phase through a calcium-dependent mechanism. *J. Comp. Physiol.*, **161**, 335–346.
- Meijer, J.H. & Schwartz, W.J. (2003) In search of the pathways for light-induced pacemaker resetting in the suprachiasmatic nucleus. *J. Biol. Rhythms*, **18**, 235–249.
- Michel, S., Itri, J. & Colwell, C.S. (2002) Excitatory mechanisms in the suprachiasmatic nucleus: The role of AMPA/KA glutamate receptors. *J. Neurophysiol.*, **88**, 817–828.
- Mikkelsen, J.D., Larsen, P.J. & Ebling, F.J. (1993) Distribution of N-methyl-D-aspartate (NMDA) receptor mRNAs in the rat suprachiasmatic nucleus. *Brain Res.*, **632**, 329–333.
- Mintz, E.M., Marvel, C.L., Gillespie, C.F., Price, K.M. & Albers, H.E. (1999) Activation of NMDA receptors in the suprachiasmatic nucleus produces light-like phase shifts of the circadian clock in vivo. *J. Neurosci.*, **19**, 5124–5130.
- Miyake, S., Sumi, Y., Yan, L., Takekida, S., Fukuyama, T., Ishida, Y., Yamaguchi, S., Yagita, K. & Okamura, H. (2000) Phase-dependent responses of Per1 and Per2 genes to a light-stimulus in the suprachiasmatic nucleus of the rat. *Neurosci. Lett.*, **294**, 41–44.
- Morin, L.P. & Allen, C.N. (2006) The circadian visual system. *Brain Res. Rev.*, **51**, 1–60.
- Moriya, T., Horikawa, K., Akiyama, M. & Shibata, S. (2000) Correlative association between N-methyl-D-aspartate receptor-mediated expression of period genes in the suprachiasmatic nucleus and phase shifts in behavior with photic entrainment of clock in hamsters. *Mol. Pharmacol.*, **58**, 1554–1562.
- Neyton, J. & Paoletti, P. (2006) Relating NMDA receptor function to receptor subunit composition: limitations of the pharmacological approach. *J. Neurosci.*, **26**, 1331–1333.
- Obrietan, K., Impey, S. & Storm, D.R. (1998) Light and circadian rhythmicity regulate MAP kinase activation in the suprachiasmatic nuclei. *Nat. Neurosci.*, **1**, 693–700.
- O'Hara, B.F., Andretic, R., Heller, H.C., Carter, D.B. & Kilduff, T.S. (1995) GABA_A, GABA_C, and NMDA receptor subunit expression in the suprachiasmatic nucleus and other brain regions. *Brain Res. Mol. Brain Res.*, **28**, 239–250.
- Pennartz, C.M.A., Hamstra, R. & Geurtsen, A.M.S. (2001) Enhanced NMDA receptor activity in retinal inputs to the rat suprachiasmatic nucleus during the subjective night. *J. Physiol. (Camb.)*, **532**, 181–194.
- Quinlan, E.M., Olstein, D.H. & Bear, M.F. (1999) Bidirectional, experience-dependent regulation of N-methyl-D-aspartate receptor subunit composition in the rat visual cortex during postnatal development. *Proc. Natl Acad. Sci. U.S.A.*, **96**, 12 876–12 880.
- Rachline, J., Perin-Dureau, F., Le Goff, A., Neyton, J. & Paoletti, P. (2005) The micromolar zinc-binding domain on the NMDA receptor subunit NR2B. *J. Neurosci.*, **25**, 308–317.
- Roenneberg, T., Daan, S. & Merrow, M. (2003) The art of entrainment. *J. Biol. Rhythms*, **18**, 183–194.
- Shibata, S. & Moore, R.Y. (1993) Neuropeptide Y and optic chiasm stimulation affect suprachiasmatic nucleus circadian function in vitro. *Brain Res.*, **615**, 95–100.
- Shibata, S., Watanabe, A., Hamada, T., Ono, M. & Watanabe, S. (1994) N-methyl-D-aspartate induces phase shifts in circadian rhythm of neuronal activity of rat SCN in vitro. *Am. J. Physiol.*, **267**, R360–R64.
- Tischkau, S.A., Mitchell, J.W., Tyan, S.H., Buchanan, G.F. & Gillette, M.U. (2003) Ca²⁺/cAMP response element-binding protein (CREB)-dependent activation of Per1 is required for light-induced signaling in the suprachiasmatic nucleus circadian clock. *J. Biol. Chem.*, **278**, 718–723.
- Travnickova-Bendova, Z., Cermakian, N., Reppert, S.M. & Sassone-Corsi, P. (2002) Bimodal regulation of mPeriod promoters by CREB-dependent signaling and CLOCK/BMAL1 activity. *Proc. Natl Acad. Sci. U.S.A.*, **99**, 7728–7733.
- de Vries, M.J., Treep, J.A. & Meijer, J.H. (1994) Electrical stimulation of the anterior optic chiasm mimics the phase shifting effects of light on the circadian activity rhythm of the Syrian hamster. *Biol. Rhythms Res.*, **25**, 211–213.
- West, A.E., Chen, W.G., Dalva, M.B., Dolmetsch, R.E., Kornhauser, J.M., Shaywitz, A.J., Takasu, M.A., Tao, X. & Greenberg, M.E. (2001) Calcium regulation of neuronal gene expression. *Proc. Natl Acad. Sci. U.S.A.*, **98**, 11 024–11 031.
- Williams, K. (1993) Ifenprodil discriminates subtypes of the N-methyl-D-aspartate receptor: selectivity and mechanisms at recombinant heteromeric receptors. *Mol. Pharmacol.*, **44**, 851–859.
- Williams, K. (2001) Ifenprodil, a novel NMDA receptor antagonist: site and mechanism of action. *Curr. Drug Targets*, **2**, 285–298.
- Yan, L., Takekida, S., Shigeyoshi, Y. & Okamura, H. (1999) Per1 and Per2 gene expression in the rat suprachiasmatic nucleus: circadian profile and the compartment-specific response to light. *Neuroscience*, **94**, 141–150.